



Numerical Study of Electro-thermo-convection in a Differentially Heated Cavity Filled with a Dielectric Liquid Subjected to Partial Unipolar Injection

W. Hassen*^a, P. Traore^b, M. N. Borjini^a, H. Ben Aissia^a

^a Department of Energetic, University of Monastir, Monastir, Tunisia

^b Department Fluid, Thermal, Combustion, Prime Institute, Futuroscope Chasseneuil, France.

PAPER INFO

Paper history:

Received 26 April 2015

Received in revised form 04 July 2015

Accepted 30 July 2015

Keywords:

Heat transfer

Electro-Hydro-Dynamic

Electro-thermo-convection

Dielectric Liquid

Numerical Simulation

ABSTRACT

The Coulomb force applied by an electric field on any charge present in a dielectric liquid may cause fluid motion. At high applied electric fields in an insulating liquid, electric charge carriers are created at metallic/liquid interfaces, a process referred to as ion injection, and result from complex electrochemical reactions. In this article we deal with the problem of electro-thermo convection in a dielectric liquid placed in a square cavity and subjected to the simultaneous action of a thermal gradient and an electric field. Thus, the aim is to analyze, from a numerical point of view, the evolution of flow structure, charge distribution and heat transfer in the case of a strong injection. The computational domain is as follow: the vertical walls are differentially heated; the horizontal walls are adiabatic except a part of the bottom wall (33% of the total length) is defined as the injecting electrodes. Three possible configurations are treated depending on the location of the injecting electrode: so we identify an injection from the left, from the middle and finally from the right. The results show that a partial injection can enhance heat transfer up to 24%. The flow structure in terms of streamlines, distribution of electric charge density and thermal field is highlighted. The effect of various system parameters in particular the injection zone locations, the electric Rayleigh number is investigated as well.

doi: 10.5829/idosi.ije.2015.28.09c.12

NOMENCLATURE

		Greek Symbols	
a	Thermal diffusivity (m ² /s)	β	coefficient of thermal expansion (K ⁻¹)
$C = \frac{q L^2}{\varepsilon \Delta V}$	Dimensionless number which measure the injection strength	ε	permittivity of the fluid (F/m)
E_x, E_y	Electric fields (V/m)	θ	Temperature (K)
g	Gravity(m/s ²)	μ	Dynamic viscosity (Pa.s)
K	ionic mobility of the liquid (m ² /V.s)	ν	kinematic viscosity (m ² /s)
L	Enclosure Width (m)	ρ	Density (kg/m ³)
$M = \frac{1}{K} \left(\frac{\varepsilon}{\rho} \right)^{0.5}$	Dimensionless number which characterizes EHD properties of the liquid	Ψ	Stream function
$Pr = \frac{\nu}{a}$	Prandtl number	ω	Vorticity
q	Electric charge density (C/m ³)	Subscripts	
$Ra = \frac{g \beta \Delta \theta L^3}{\nu a}$	Thermal Rayleigh number	f	Cold
t	Time (s)	c	Hot
$T = \frac{\varepsilon \Delta V}{\rho \nu K}$	Electric Rayleigh number	superscripts	
U_x, U_y	horizontal and vertical velocity (m/s)	'	dimensional variable
V	electricpotential (V)		

*Corresponding Author's Email: hassen.walid@gmail.com (W. Hassen)

1. INTRODUCTION

The problem of natural convection in cavities [1-3] has been thoroughly investigated in the past. Less studies are concerned with combined electric and buoyancy forces, but this new topic becomes more and more active [4-7]. The complexities of the observed phenomena when a thermal gradient and an electric field are applied simultaneously in a dielectric liquid layer have received much attention in recent years.

The richness of behaviors observed in this particular configuration is mainly due to the secondary flow induced by unipolar injection of electric charges. This secondary motion causes the interest of many specialized sections of the scientific and industrial communities. One of the greatest interest for such studies, results from the significant enhancement of heat transfer which has been observed in such situations. Indeed, charge injection may be viewed as an interesting technique to improve the rate of heat transfer and to increase demands for smaller and more efficient thermal systems. Most of the authors who have dealt with the problem of electro-convection, have tackled the problem with the stability theory [8-12].

Atten et al. [13, 14] have presented experimental studies in the case of the Rayleigh Benard configuration where the fluid is heated from the bottom. They showed that the agitation induced by the Coulomb force resulting from unipolar injection has a major influence on heat transfer. They also tried to correlate the increase of the Nusselt number to electric quantities such as (injection current, electric potential) and to the geometry of the domain (essentially the distance between the two metallic electrodes). They found a report of proportionalities very satisfactory.

In [15, 16], Vazquez et al. have solved numerically the problem of isothermal electroconvection. Two different methods (finite elements combined with the particle-in-cell method "FE-PIC" and finite elements and the flux-corrected transport method "FE-FCT") have been compared. The resolution is in fact not entirely numerical, because one imposes in these methods the distribution of velocity for each node. They treated the case of strong and weak injection, and investigated the structure of the flow and the electric charge density distribution. Pure numerical work which solves the coupled equations defining the problem is very rare. Recently, Traore et al. [17-20] solved numerically, for the first time, the entire set of equations associated to the electro-thermo-convective phenomena that takes place in a planar (and annular) layer of dielectric liquid heated from below and subjected to unipolar injection. They analyzed the relation between fluid velocity, electrical Rayleigh number T , thermal Rayleigh number Ra and Prandtl number Pr . They also computed the heat transfer enhancement due to the

electric field. In the present paper, the numerical simulation of the electro-thermo-convective liquid motion in square enclosure is presented. We consider here the unipolar ion injection from (whole or part) of the metallic electrode into a dielectric liquid of low conductivity. We solve the entire set of coupled conservation equations (mass, momentum, electric charge and potential) directly using an efficient control-volume method. We focus on the evolution of the flow, the distribution of electric charge density, the profile of the streamlines and the development of thermal field. The influence of the induced electro-convection on the heat transfer is studied and analyzed in detail.

2. MATHEMATICAL FORMULATION AND NUMERICAL MODEL

We consider a dielectric liquid layer confined in a square cavity of length L . The two vertical walls are maintained respectively at fixed temperatures θ_c and θ_f . On the two other adiabatic walls, electrodes are flushed. The emitter electrode corresponding to all or to part of the bottom wall (33% of the total length) is held at potential V_0 and represents the source of ions injection. The collector electrode is flushed on the entire top wall and is designed to absorb these injected ions and it is held at potential V_1 .

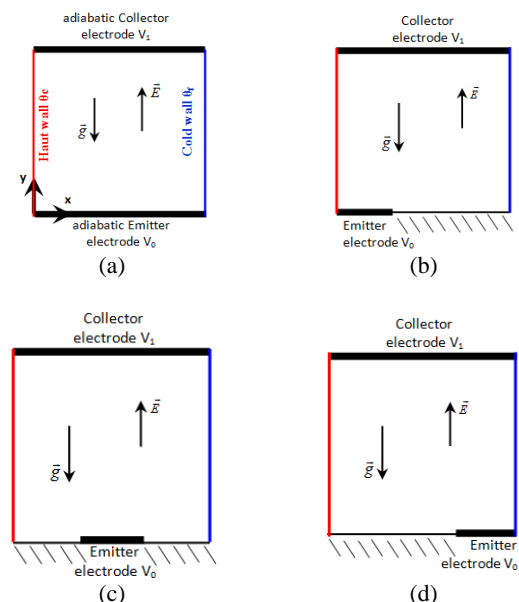


Figure 1. Geometry of the various configurations studied. (a): Total injection, (b): Partial injection from the left, (c): Partial injection from the middle, (d): Partial injection from the right.

The layer is thus subjected simultaneously to a thermal difference $\Delta\theta=\theta_c-\theta_f$ and a potential difference $\Delta V=V_0-V_1$. Four possible configurations (Figure 1) are treated depending on the location of the injection zone: so we identify a total injection, a partial injection from the left, the middle and finally from the right side of the bottom wall. The problem is formulated considering the usual hypotheses of Newtonian and incompressible fluid of kinematics viscosity “ ν ”, density “ ρ ”, permittivity “ ε ” and thermal diffusivity “ a ”. The injection of unipolar charge of mobility “ K ” at the emitter is assumed ‘homogeneous’ and ‘autonomous’; this means that q_0 the injected charge at the emitter electrode is assumed to be constant and independent of the local electric field. In addition, to avoid excessive complexity, we neglect Joule heating. Finally we consider the Boussinesq approximation. The general set of equations expressing the conservation of mass and momentum (the Navier-Stokes equations) including electrical and buoyancy forces, energy conservation, charge density conservation, the Gauss theorem and the definition of the electric field towards electric potential V , takes the form :

$$\nabla \cdot \vec{U}' = 0 \tag{1}$$

$$\rho_0 \left(\frac{\partial \vec{U}'}{\partial t'} + (\vec{U}' \cdot \nabla) \vec{U}' \right) = -\nabla P' + \mu \left(\frac{\partial^2 \vec{U}'_i}{\partial x_i'^2} + \frac{\partial^2 \vec{U}'_j}{\partial x_j'^2} \right) + \vec{f}' + \rho_0 \beta (\theta' - \theta_0) \tag{2}$$

$$\rho_0 C_p \left(\frac{\partial \theta'}{\partial t'} + \vec{U}' \cdot \nabla \theta' \right) = \nabla \cdot (\lambda \nabla \theta') \tag{3}$$

$$\frac{\partial q'}{\partial t'} + \nabla \cdot \vec{j}' = 0 \tag{4}$$

$$\nabla \cdot (\varepsilon \vec{E}') = q' \tag{5}$$

$$\vec{E}' = -\nabla V' \tag{6}$$

In Equation (2) \vec{f}' is the electric force

$$\vec{f}' = q' \vec{E}' - \frac{1}{2} E'^2 \nabla \varepsilon + \nabla \left(\frac{1}{2} \rho E'^2 \left(\frac{\partial \varepsilon}{\partial q'} \right)_\theta \right) \tag{7}$$

In Equation (4) \vec{j}' represents the current density which is defined as:

$$\vec{j}' = q' (\vec{U}' + K \vec{E}') \tag{9}$$

In Equation (7), the first term known as Coulomb force, is the force per unit volume exerted by electric field on a medium containing free charges. Under D.C. conditions, the second term corresponds to the dielectric force and it is very weak compared to the Coulomb force.

The third term which represents the effect of electrostriction has the gradient form and can be included in the pressure term of momentum equation, but in the case of incompressible fluid this term can be also neglected [21-23]. Thus, finally the electric force can be expressed as:

$$\vec{f}' = q' \vec{E}' \tag{9}$$

As numerical method we had recourse to the “Vorticity - Stream function” formalism ($\psi-\omega$), which allows the elimination of the pressure which is always tricky to handle in case of incompressible fluids.

They are respectively defined by the two following relations:

$$\vec{\omega}' = \nabla \times \vec{u}' \tag{10}$$

And

$$\vec{u}' = \nabla \times \vec{\psi}' \tag{11}$$

Introducing the following dimensionless variables:

$$\begin{aligned} x &= \frac{x'}{L} & y &= \frac{y'}{L} & U_x &= U'_x \frac{L}{a} & U_y &= U'_y \frac{L}{a} \\ \psi &= \frac{\Psi'}{a} & \omega &= \omega' \frac{L^2}{a} & t &= t' \frac{a}{L^2} & \theta &= \frac{(\theta' - \theta_f)}{(\theta_c - \theta_f)} & q &= \frac{q'}{q_0} \\ E &= E' \frac{L}{(V_0 - V_1)} & v &= \frac{(V' - V_1)}{(V_0 - V_1)} \end{aligned}$$

That leads to the definition of the following dimensionless numbers:

$$T = \frac{\varepsilon \Delta V}{\rho \nu K}, \quad C = \frac{q_i (r_0 - r_1)^2}{\varepsilon \Delta V} \quad \text{and} \quad M = \frac{1}{K} \sqrt{\frac{\varepsilon}{\rho}}$$

which are respectively the ratio between the Coulomb and the viscous forces (called electric Rayleigh number), the measure of the injection strength and the mobility parameter which accounts for electro-hydrodynamic properties of the liquid.

For a two-dimensional geometry the system which governs this type of electro-thermo-convective flow (1) - (6) is written in dimensionless form as:

$$\omega = - \left(\frac{\partial^2 \Psi}{\partial x^2} + \frac{\partial^2 \Psi}{\partial y^2} \right) \tag{12}$$

$$\begin{aligned} \frac{\partial \omega}{\partial t} + U_x \frac{\partial \omega}{\partial x} + U_y \frac{\partial \omega}{\partial y} &= \frac{\partial^2 \omega}{\partial x^2} + \frac{\partial^2 \omega}{\partial y^2} + \text{Ra.Pr} \frac{\partial \theta}{\partial x} \\ &+ \frac{CT^2}{M^2} \cdot \text{Pr}^2 \left(\frac{\partial (q E_y)}{\partial x} - \frac{\partial (q E_x)}{\partial y} \right) \end{aligned} \tag{13}$$

$$\frac{\partial \theta}{\partial t} + U_x \frac{\partial \theta}{\partial x} + U_y \frac{\partial \theta}{\partial y} = \left(\frac{\partial^2 \theta}{\partial x^2} + \frac{\partial^2 \theta}{\partial y^2} \right) \tag{14}$$

$$\frac{\partial q}{\partial t} + \frac{\partial}{\partial x} \left(q \left(U_x + \frac{T \text{ Pr}}{M^2} E_x \right) \right) + \frac{\partial}{\partial y} \left(q \left(U_y + \frac{T \text{ Pr}}{M^2} E_y \right) \right) = 0 \tag{15}$$

$$\frac{\partial^2 V}{\partial x^2} + \frac{\partial^2 V}{\partial y^2} = -C \cdot q \quad (16)$$

$$E_x = -\frac{\partial V}{\partial x} \quad (17)$$

$$E_y = -\frac{\partial V}{\partial y} \quad (18)$$

The associated initial and boundary conditions for the problem considered are as follow:

- For $t=0$:

$$\omega = \Psi = \frac{\partial \Psi}{\partial y} = \frac{\partial \Psi}{\partial x} = \theta = V = q = 0 \text{ everywhere} \quad (19)$$

- For $t>0$

Hot wall ($x=0$)

$$\Psi = \frac{\partial \Psi}{\partial y} = 0; \theta = 1; \frac{\partial q}{\partial y} = \frac{\partial V}{\partial y} = 0; \omega = -\frac{\partial^2 \Psi}{\partial x^2} \quad (20)$$

Cold wall ($x=L$)

$$\Psi = \frac{\partial \Psi}{\partial y} = 0; \theta = 0; \frac{\partial q}{\partial y} = \frac{\partial V}{\partial y} = 0; \omega = -\frac{\partial^2 \Psi}{\partial x^2} \quad (21)$$

Bottom wall ($y=0$)

At the injector

$$\Psi = \frac{\partial \Psi}{\partial x} = 0; \frac{\partial \theta}{\partial y} = 0; q = 1; V = 1 \quad (22)$$

Out of the injector

$$\Psi = \frac{\partial \Psi}{\partial x} = 0; \frac{\partial \theta}{\partial y} = 0; \frac{\partial q}{\partial y} = \frac{\partial V}{\partial y} = 0 \quad (23)$$

Top wall ($y=L$)

$$\Psi = \frac{\partial \Psi}{\partial x} = 0; \frac{\partial \theta}{\partial y} = 0; \frac{\partial q}{\partial y} = 0; V = 0 \quad (24)$$

The partial differential Equations (12)-(18) governing the EHD flow field and the associate boundary condition (19)-(24) are integrated over a control volume. Due to stability contingencies and in order to prevent excessive numerical diffusion the power-law scheme for treating convective terms [24] is chosen, also a semi-implicit first order Euler time scheme is retained to discretize the temporal derivatives [25].

One obtains a set of algebraic equations for the vorticity, stream function, energy, charge density and electric potential. These algebraic set of equations are solved using Successive Over Relaxation (SOR) based on the Gauss- Seidel iterative solver [26].

The choice of the relaxation coefficients for each unknown Ψ , ω , V , θ and q depends mainly on electric Rayleigh number. At high electric Rayleigh number to avoid the divergence of the computation Ψ , ω , V , θ and q are under-relaxed. At low electric Rayleigh number in

order to accelerate the calculation, Ψ is over relaxed whereas ω , V , θ and q are under-relaxed.

Grid independency checks were performed and a 51 x 51 control volumes were found sufficient enough for the desired accuracy. Finer meshes have been tested without showing greater improvement of the results. The non-dimensional time step was chosen equal to 10^{-4} which ensured the stability of the computations [15].

The stopping criterion is satisfied as soon as $\frac{\max|\psi^k - \psi^{k-1}|}{\max|\psi^k|} + \max|q^k - q^{k-1}| \leq 10^{-5}$ for each time step,

where the superscript k designates the k^{th} iteration of the SOR algorithm. For additional information on the numerical method, the reader may refer to the article by Hassen et al. [18-20]. Finally, it is also noted that the dimensionless parameters used for these simulations are: $Ra = 10000$, $Pr=10$, $M=10$ (corresponding to the liquid gasoil), $C = 10$ corresponding to the strong injection case and T varies between 200 and 1200.

3. RESULTS AND DISCUSSION

3. 1. Validation Tests and Choice of Mesh Size

The code has been validated by several comparisons between numerical results and theoretical ones. The accuracy of the numerical method is carefully analyzed through various grid sizes.

In Table 1, we have presented the comparison between the analytical and numerical profiles of charge density obtained in the case of an isothermal steady hydrostatic solution.

To obtain this solution numerically, we solved Equations (12-13) and (15-16) while keeping the vorticity to zero (to be in hydrostatic case) and running the code for a value of T below the critical value T_c for which the instability starts to grow.

The analytical hydrostatic solution for the charge density is $q(y) = \frac{i}{2C}(y+j)^{-\frac{1}{2}}$. For $C=10$ the values of i , j , and k are: $i=1.4882$, $j=5.539 \cdot 10^{-3}$ and $k = 1.0004$ [27].

A good agreement is found even for a relatively coarse mesh, but for more precision and smoother results we opted for a mesh of 51x51.

3. 2. Effect of the Electric Field on the Charge Density

The distribution of the charge density shows that the greatest concentration of electric charge remains close to the emitter electrode, Due to the Coulomb force and the potential difference between the two electrodes, electro-plumes arise. We note that the charge density drops by 50% after crossing only 3% of the cavity length and for the case of a partial injection, we have not only a longitudinal migration toward the receiving electrode but we also observe a transverse

migration. For a weak electric Rayleigh (Figure 2 a, c and d) the electric charges migration reaches the top wall but only from the left side of wall. Indeed, these electric charges are carried and dominated by the flow due to buoyancy force. By increasing the electric Rayleigh (Figure 2 e, g and h) the competition between the ascending thermal forces and descending electric forces (near the right vertical wall) tilts in favor of the electric forces which allows the creation of a second electric charge migration flows in the right side.

In the case of left partial injection (Figure 2 b and f) the position of the injecting electrode is such that both thermal and electrical forces can only cooperate. This allows to have whatever the value of the electric Rayleigh number, an electro-plume located just in the side of the hot wall.

TABLE 1. Charge density value corresponding to the analytical steady hydrostatic solution

y	analytical solution	Charge density q (error %)			
		Numerical solution for different mesh size			
		31x31	41x41	51x51	61x61
0.001	0.920	0.953 (03.60%)	0.941 (2.23%)	0.925 (0.52%)	0.922 (0.27%)
0.01	0.596	0.633 (06.22%)	0.610 (2.42%)	0.601 (0.77%)	0.598 (0.32%)
0.05	0.315	0.343 (08.78%)	0.324 (2.81%)	0.318 (0.89%)	0.316 (0.39%)
0.1	0.229	0.257 (12.11%)	0.236 (3.14%)	0.231 (0.95%)	0.230 (0.45%)
0.2	0.164	0.185 (12.54%)	0.170 (3.47%)	0.166 (1.08%)	0.165 (0.49%)
0.4	0.116	0.131 (13.21%)	0.120 (3.46%)	0.117 (1.11%)	0.117 (0.58%)
0.6	0.095	0.108 (13.67%)	0.099 (3.95%)	0.096 (1.23%)	0.096 (0.67%)
0.8	0.083	0.094 (14.34%)	0.085 (4.22%)	0.0841 (1.33%)	0.0836 (0.75%)
1	0.074	0.085 (14.75%)	0.077 (4.39%)	0.0751 (1.52%)	0.0746 (0.77%)

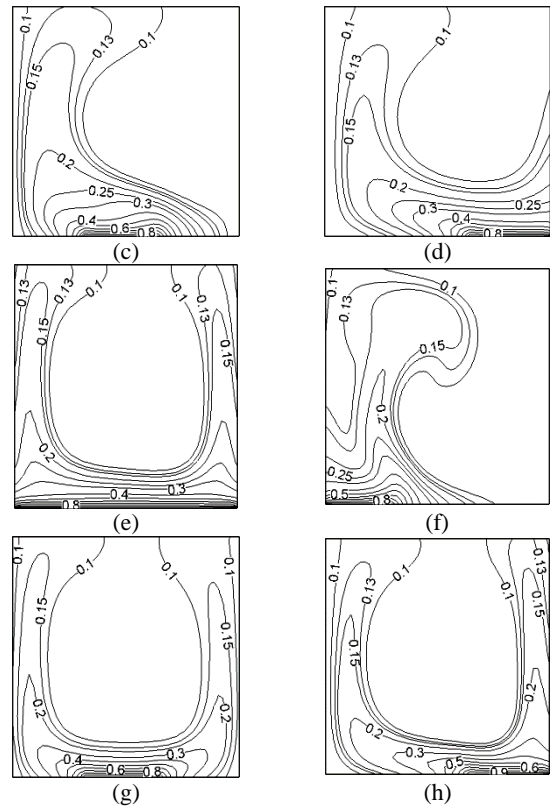


Figure 2. Isocontours of the electric charge density of for $Pr=10$, $Ra=10^4$, $C=10$ and $M=10$. (a), (b), (c) and (d) are respectively: Total injection, partial left injection, partial middle injection and partial right injection for $T=200$. (e), (f), (g) and (h) are respectively: Total injection, partial left injection, partial middle injection and partial right injection for $T=500$.

3. 3. Effect of the Electric Field on the Flow Structure

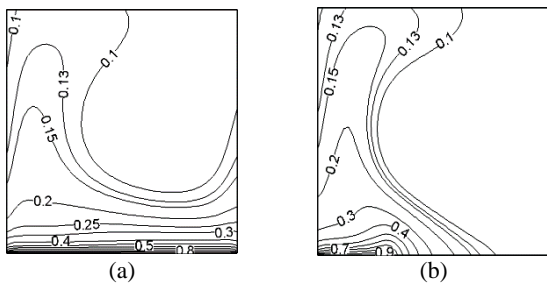
We obtain a large circulation buckle comprising a clockwise rotating single cell which occupies the entire cavity.

We also note that the structure of the vortex has an elliptical shape in the longitudinal direction and its angular velocity is low.

Starting the injection from the bottom electrode ($T=200$, Figure 3b, 3c, 3d and 3e) it is clear that the electric and thermal fields are acting in the same direction as shown in Figures 2a, 2b, 2c and 2d. These latter fields generate a sudden acceleration of the angular velocity of the cell (which has almost doubled).

The flow structure has not changed except the shape of the vortex which becomes circular. The location of the injector plane has no significant effect on this structure.

In Figures 3f, 3h and 3i, the electric field is so important ($T=500$) that we notice the existence of a secondary counter rotating cell which appears and grows in the domain.



The first cell near the hot wall (left) is more impressive because it is due to the combination of both thermal and electrical forces. The second one near the cold wall (right) is due to the competition between the descending thermal force and ascending Coulomb force. This competition promotes finally the electric force that allows the creation of this counter rotating cell.

For a partial left injection shown in Figure 3 g next to the main central cell, two cells arise near the upper and lower left corners. The central cell has increased its angular velocity 5 times compared to the case for $T = 200$.

3. 4. Effect of the Electric Field on Heat Transfer

Heat transfer can be characterized by the local and average Nusselt numbers. The average Nusselt numbers versus the type of injector configuration and T number are given in Table 2.

First it is worth noting that heat transfer improves with the increase of electric Rayleigh number except around $T= 400$ for the cases of Total injection, Partial middle injection and Partial right injection. The decrease of the Nusselt number was expected, since at $T = 400$ a second counter-rotating cell arises. This leads to a segmentation which greatly hampers the heat transfer.

The partial right injection has to be avoided because it gives the worst average Nusselt number. For $T < 300$ the best heat exchange corresponds to the partial middle injection case, while for $T > 300$ heat transfer is better for the case of partial left injection.

This result is supported by Figures 4a and 4b, which present the local Nusselt number on hot wall.

This figure depicts the increase of local Nusselt number when the electric Rayleigh is greater. We clearly see that the heat transfer is more important at the bottom of the hot wall in particular for Y between 0.2 and 0.4

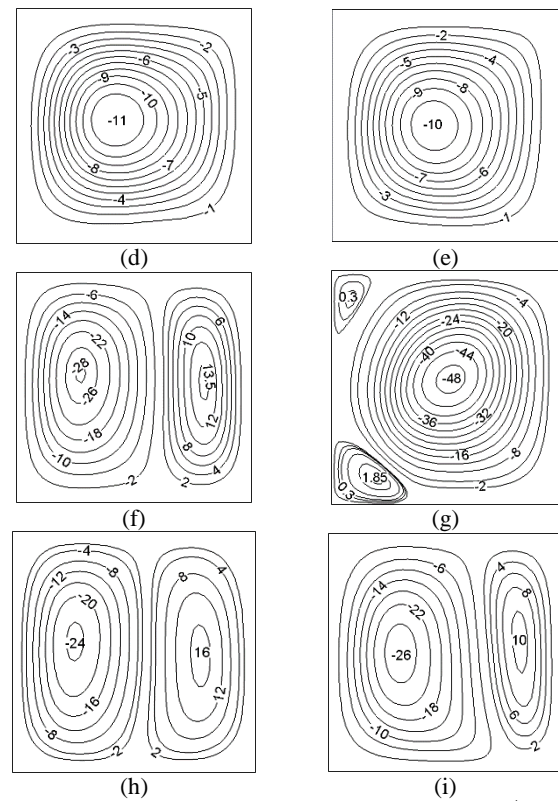
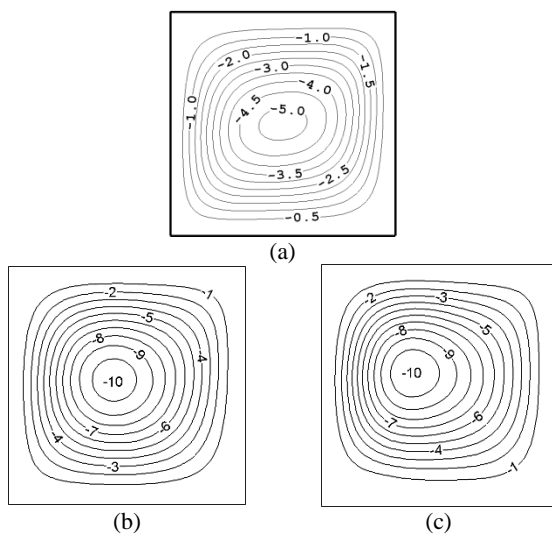


Figure 3. Caption of stream lines for $Pr=10, Ra=10^4, C=10$ and $M= 10$.

(a): without injection $T= 0$. (b), (c), (d) and (e) are respectively: Total injection, partial left injection, partial middle injection and partial right injection for $T=200$. (f), (g), (h) and (i) are respectively: Total injection, partial left injection, partial middle injection and partial right injection for $T=500$.

TABLE 2. Average Nusselt number as function of electric Rayleigh and the position of the injector plane ($Pr =10, Ra=10^4, C= 10$ and $M= 10$)

T	Average Nu			
	Total injection	Partial left injection	Partial middle injection	Partial right injection
150	2.58	2.60	2.65	2.54
175	2.64	2.68	2.72	2.60
200	2.71	2.76	2.82	2.66
250	2.82	2.91	2.99	2.76
275	2.86	2.98	3.14	2.79
300	2.89	3.06	3.19	2.78
400	2.51	3.13	2.52	2.34
500	3.00	3.38	3.10	2.90
800	4.05	4.42	4.07	4.06
1200	5.19	5.70	5.42	5.19



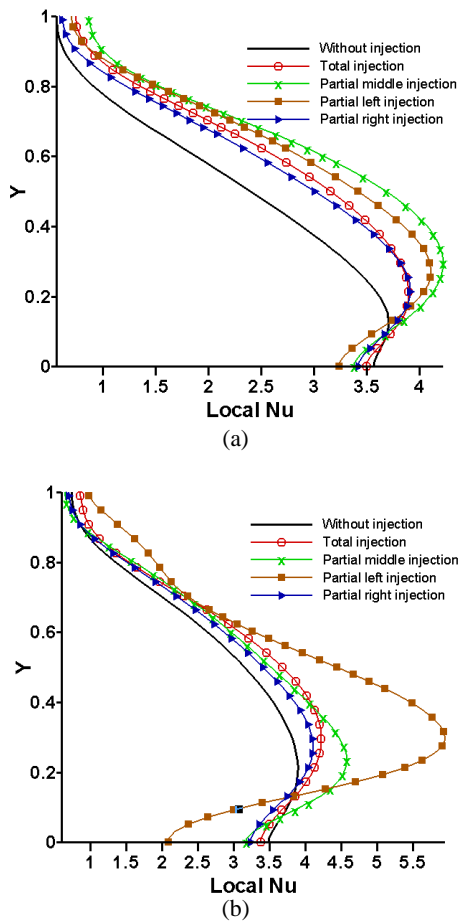


Figure 4. Variation of the local Nusselt number on the hot wall for $Pr = 10$, $Ra = 10^4$, $C = 10$ and $M = 10$. (a) : $T = 200$, (b): $T = 500$.

4. CONCLUSION

A two-dimensional numerical study has been performed to investigate the effect of the partial electric charge injection on heat transfer and fluid flow structure in a differentially heated square enclosure. The whole coupled set of hydro, thermo and electro dynamic equations have been solved using the control-volume method.

The effects of the injection zone locations as well as electric Rayleigh number are investigated. Important findings can be drawn from this work as listed below: The injection of electric charge enhances significantly the heat transfer.

The partial right injection location has to be avoided because it gives the worst average Nusselt number, stating a weak enhancement of heat transfer.

The partial right injection location has to be avoided because it gives the worst average Nusselt number, stating a weak enhancement of heat transfer. For moderate electric Rayleigh numbers ($T \leq 300$), the middle injection gives the best increase of heat transfer while for higher values ($T > 300$) the left-sided injection has to be recommended.

5. REFERENCES

- Maatki, C., Ghachem, K., Kolsi, L., Borjini, M. and Aissia, H.B., "Entropy generation of double diffusive natural convection in a three dimensional differentially heated enclosure", *International Journal of Engineering-Transactions B: Applications*, Vol. 27, No. 2, (2013), 215-226.
- Saha, G., Saha, S., Hasan, M. and Islam, M.Q., "Natural convection heat transfer within octagonal enclosure", *IJE Transactions A: Basics*, Vol. 23, No. 1, (2010), 1-10.
- Sheikhzadeh, G., Arefmanesh, A., Kheirkhah, M. and Abdollahi, R., "Numerical study of natural convection in an inclined cavity with partially active side walls filled with cu-water nanofluid", *International Journal of Engineering-Transactions B: Applications*, Vol. 24, No. 3, (2011), 279-292.
- Traore, P., Wu, J., Perez, A., Romat, H., Koulova, D. and Louste, C., "Heat transfer enhancement induced by electrically generated convection in a plane layer of dielectric liquid", in *Journal of Physics: Conference Series*, IOP Publishing. Vol. 395, (2012), 012127.
- Koulova, D., Romat, H. and Traore, P., "Flow patterns and heat transfer in electro-thermo-convection", in *Journal of Physics: Conference Series*, IOP Publishing. Vol. 395, (2012), 012104.
- Dantchi, K., Philippe, T., Hubert, R., Jian, W. and Christophe, L., "Numerical simulations of electro-thermo-convection and heat transfer in 2d cavity", *Journal of Electrostatics*, Vol. 71, No. 3, (2013), 341-344.
- Saidi, M. and Moradian, A., "Availability analysis for heterogeneous nucleation in a uniform electric field", *International Journal of Engineering-Transactions A: Basics*, Vol. 16, No. 2, (2003), 205-216.
- Pontiga, F. and Castellanos, A., "Galerkin analysis of electrothermal instabilities in plane liquid layers", *Industry Applications, IEEE Transactions on*, Vol. 30, No. 4, (1994), 862-876.
- Pontiga, F. and Castellanos, A., "The onset of electrothermal convection in nonpolar liquids on the basis of a dissociation-injection conductivity model", *Industry Applications, IEEE Transactions on*, Vol. 28, No. 3, (1992), 520-527.
- Pontiga, F. and Castellanos, A., "Physical mechanisms of instability in a liquid layer subjected to an electric field and a thermal gradient", *Physics of Fluids*, Vol. 6, No. 5, (1994), 1684-1701.
- Castellanos, A., Atten, P. and Velarde, M., "Oscillatory and steady convection in dielectric liquid layers subjected to unipolar injection and temperature gradient", *Physics of Fluids (1958-1988)*, Vol. 27, No. 7, (1984), 1607-1615.
- Rodriguez-Luis, A., Castellanos, A. and Richardson, A., "Stationary instabilities in a dielectric liquid layer subjected to an arbitrary unipolar injection and an adverse thermal gradient", *Journal of Physics D: Applied Physics*, Vol. 19, No. 11, (1986), 2115.
- Atten, P., McCluskey, F. and Perez, A., "Electroconvection and its effect on heat transfer", *Electrical Insulation, IEEE Transactions on*, Vol. 23, No. 4, (1988), 659-667.
- Atten, P., McCluskey, F. and Perez, A., "Augmentation du transfert thermique par electroconvection", *Revue de Physique Appliquée*, Vol. 22, No. 9, (1987), 1095-1101.
- Vazquez, P., Georghiou, G. and Castellanos, A., "Numerical analysis of the stability of the electrohydrodynamic (ehd) electroconvection between two plates", *Journal of Physics D: Applied Physics*, Vol. 41, No. 17, (2008), 175303.
- Vazquez, P., Georghiou, G. and Castellanos, A., "Characterization of injection instabilities in electrohydrodynamics by numerical modelling: Comparison of

- particle in cell and flux corrected transport methods for electroconvection between two plates", *Journal of Physics D: Applied Physics*, Vol. 39, No. 13, (2006), 2754-2763.
17. Traore, P., Perez, A., Koulova, D. and Romat, H., "Numerical modelling of finite-amplitude electro-thermo-convection in a dielectric liquid layer subjected to both unipolar injection and temperature gradient", *Journal of Fluid Mechanics*, Vol. 658, (2010), 279-293.
 18. Hassen, W., Borjini, M.N. and Aissia, H.B., "Enhanced heat transfer by unipolar injection of electric charges in differentially heated dielectric liquid layer", *FDMP: Fluid Dynamics & Materials Processing*, Vol. 8, No. 4, (2012), 381-396.
 19. Hassen, W., Borjini, M., Traore, P. and Aissia, H.B., "Electroconvection between coaxial cylinders of arbitrary ratio subjected to strong unipolar injection", *Journal of Electrostatics*, Vol. 71, No. 5, (2013), 882-891.
 20. Hassen, W., Elkhazen, M.I., Traore, P. and Borjini, M.N., "Numerical study of the electro-thermo-convection in an annular dielectric layer subjected to a partial unipolar injection", *International Journal of Heat and Fluid Flow*, Vol. 50, No., (2014), 201-208.
 21. Atten, P. and Moreau, R., "Stabilitee electrohydrodynamique des liquides isolants soumis à une injection unipolaire", *J. Mécanique*, Vol. 11, No. 3, (1972), 471-521.
 22. Atten, P. and Lacroix, J., "Non-linear hydrodynamic stability of liquids subjected to unipolar injection", *Journal de Mécanique*, Vol. 18, (1979), 469-510.
 23. El Moctar, A.O., Peerhossaini, H., Le Peurian, P. and Bardou, J., "Ohmic heating of complex fluids", *International Journal of Heat and Mass Transfer*, Vol. 36, No. 12, (1993), 3143-3152.
 24. Patankar, S., "Numerical heat transfer and fluid flow, CRC Press, (1980).
 25. Borjini, M.N., Abidi, A. and Aissia, H.B., "Prediction of unsteady natural convection within a horizontal narrow annular space using the control-volume method", *Numerical Heat Transfer, Part A: Applications*, Vol. 48, No. 8, (2005), 811-829.
 26. Bejan, A., "Convection heat transfer, John Wiley & sons, (2013).
 27. Wu, J., "Contribution to numerical simulation of electrohydrodynamics flows: Application to electro-convection and electro-thermo-convection between two parallel plates", Poitiers, (2012),

Numerical Study of Electro-thermo-convection in a Differentially Heated Cavity Filled with a Dielectric Liquid Subjected to Partial Unipolar Injection

W. Hassen ^a, P. Traore ^b, M.N. Borjini ^a, H. Ben Aissia ^a

^a Department of Energetic, University of Monastir, Monastir, Tunisia

^b Department Fluid, Thermal, Combustion, Prime Institute, Futuroscope Chasseneuil, France.

PAPER INFO

چکیده

Paper history:

Received 26 April 2015

Received in revised form 04 July 2015

Accepted 30 July 2015

Keywords:

Heat transfer

Electro-Hydro-Dynamic

Electro-thermo-convection

Dielectric Liquid

Numerical Simulation

نیروی کولن در یک مایع دی الکتریک بر روی هر ذره باردار توسط یک میدان الکتریکی ممکن است موجب حرکت سیال شود. در میدان‌های الکتریکی شدید وارد شده بر یک عایق حرارتی مایع، حامل‌های بار الکتریکی در فصل مشترک فلز/مایع ایجاد می‌شوند. این فرایند به عنوان تزریق یون شناخته شده، و در نتیجه واکنش‌های پیچیده الکتروشیمیایی است. در این مقاله ما مساله همرفت الکترو-حرارتی در یک مایع دی الکتریک قرار داده شده در حفره مربع شکل و در معرض هم‌زمان شیب حرارتی و میدان الکتریکی را بررسی می‌کنیم. بنابراین، هدف تحلیل عددی تکامل ساختار جریان، توزیع بار و انتقال حرارت در مورد تزریق قوی است. دامنه محاسبات به شرح زیر است: دیوارهای عمودی در دماهای متفاوت هستند و دیوار افقی آدیاباتیک به جز بخشی از دیوار پایین (۲۳٪ از کل طول) به عنوان الکتروود تزریق تعریف شده است. بسته به محل الکتروود سه حالت تزریق ممکن است: تزریق از سمت چپ، از وسط و در نهایت از سمت راست. نتایج نشان می‌دهد که تزریق جزئی می‌تواند انتقال حرارت را تا ۲۴ درصد افزایش دهد. ساختار جریان از نقطه نظر خطوط جریان، توزیع چگالی بار الکتریکی و میدان حرارتی مورد توجه است. اثر پارامترهای سیستم‌های مختلف به ویژه در مکان‌های منطقه تزریق، عدد ریلی الکتریکی نیز بررسی شده است

doi: 10.5829/idosi.ije.2015.28.09c.12